

SCIENTIFIC REPORTS



OPEN

20S immunoproteasomes remove formaldehyde-damaged cytoplasmic proteins suppressing caspase-independent cell death

Sara Ortega-Atienza, Casey Krawic, Lauren Watts, Caitlin McCarthy, Michal W. Luczak & Anatoly Zhitkovich 

Immunoproteasomes are known for their involvement in antigen presentation. However, their broad tissue presence and other evidence are indicative of nonimmune functions. We examined a role for immunoproteasomes in cellular responses to the endogenous and environmental carcinogen formaldehyde (FA) that binds to cytosolic and nuclear proteins producing proteotoxic stress and genotoxic DNA-histone crosslinks. We found that immunoproteasomes were important for suppression of a caspase-independent cell death and the long-term survival of FA-treated cells. All major genotoxic responses to FA, including replication inhibition and activation of the transcription factor p53 and the apical ATM and ATR kinases, were unaffected by immunoproteasome inactivity. Immunoproteasome inhibition enhanced activation of the cytosolic protein damage sensor HSF1, elevated levels of K48-polyubiquitinated cytoplasmic proteins and increased depletion of unconjugated ubiquitin. We further found that FA induced the disassembly of 26S immunoproteasomes, but not standard 26S proteasomes, releasing the 20S catalytic immunoproteasome. FA-treated cells also had higher amounts of small activators PA28 $\alpha\beta$ and PA28 γ bound to 20S particles. Our findings highlight the significance of nonnuclear damage in FA injury and reveal a major role for immunoproteasomes in elimination of FA-damaged cytoplasmic proteins through ubiquitin-independent proteolysis.

Aging, reactive metabolites and other factors promote formation of misfolded and damaged proteins, which is detrimental to cell functions and is a cause of many neurodegenerative diseases¹. Proteasome-mediated degradation is the main process for elimination of damaged proteins in human cells². Proteasomes consist of two main components: the catalytic 20S core particle and the 19S regulator particle which together form the 26S proteasome. The 19S complex binds polyubiquitinated proteins, unfolds them using ATP, and feeds the unfolded polypeptide into the interior of the barrel-shaped 20S particle for proteolysis. Small activators such as PA28 $\alpha\beta$, PA28 γ and PA200 do not require ATP or ubiquitin to stimulate protein degradation by the 20S proteasome³. The 20S core particle contains three active subunits with caspase-, trypsin- and chymotrypsin-like activities. These subunits are replaced by related proteases LMP2, LMP10 (MECL1) and LMP7 in immunoproteasomes (i-proteasomes) that are the most abundantly expressed in lymphoid tissues^{4,5}. This exchange of proteolytic activities makes i-proteasomes more efficient at the generation of peptides for antigen presentation^{6,7}. Expression of i-proteasomes in all major tissues and especially in the immunoprivileged sites, such as the retina^{8,9} and brain^{9,10}, points to i-proteasome functions that are different from antigen presentation. One of these functions can involve responses to protein-damaging conditions, as evidenced by the upregulation of i-proteasomes by nitric oxide¹¹ and their role in removal of oxidized proteins^{12,13}. Enhanced abilities of i-proteasomes in degradation of basic proteins are also important for removal of the excess of free histones¹⁴.

Formaldehyde (FA) is a reactive chemical that is ubiquitously produced in cells during several normal biochemical reactions¹⁵. These endogenous processes generate biologically significant levels of FA, as evidenced by recent mouse studies in which the loss of a maternal FA detoxification enzyme produced severe growth problems in embryos¹⁶ and degenerative and genotoxic effects in the tissues of adult animals¹⁷. The metabolic production of FA is also responsible for neurotoxic effects in victims of methanol poisoning^{18,19}. FA is a common environmental

Department of Pathology and Laboratory Medicine, Brown University, Providence, RI, 02912, USA. Correspondence and requests for materials should be addressed to A.Z. (email: anatoly_zhitkovich@brown.edu)

toxicant with many sources of exposure, such as tobacco smoking²⁰, off-gassing from consumer goods and emissions by combustion processes¹⁵. Inhalation FA exposures are linked with higher risks for respiratory²¹ and other cancers^{22,23}. FA carcinogenicity is commonly associated with the formation of genotoxic DNA-protein crosslinks (DPCs) involving histones^{15,21} due to conjugation of FA with the abundant Lys ϵ -amino groups within these proteins. Protein damage by FA is quite extensive, as evidenced by a rapid heat shock response and extensive protein polyubiquitination²⁴. Vulnerability of the nervous system to toxic effects of FA^{18,19,25} is consistent with its protein-damaging properties.

Here we examined whether i-proteasomes are involved in responses to FA damage, considering that they display higher activities toward basic proteins¹⁴. We found that FA triggered the disassembly of 26S i-proteasomes promoting ubiquitin-independent removal of damaged cytoplasmic proteins and suppressing long-term cytotoxic effects. Thus, one of the nonimmune functions of i-proteasomes is protection against proteotoxicity by ubiquitinous FA and possibly by other aldehydes. Our findings are also important for the mechanistic understanding of FA toxicities, demonstrating that protein damage outside the nucleus contributes to the development of adverse effects.

Results

Gene expression of i-proteasome subunits. We selected human lung H460 and IMR90 cells as our biological models, which we have used in the past for the characterization of genotoxic signaling and proteotoxicity by FA^{24,26,27}. Based on gene expression by qRT-PCR, i-proteasomal components constituted 28.7% of all catalytic subunits in H460 cells and 16% in IMR90 cells (Fig. 1A). In both cell lines, LMP7 accounted for approximately 15–20% of $\beta 5$ subunits with chymotrypsin-like activity, which is the main proteolytic activity of proteasomes. Acute and chronic FA treatments of normal IMR90 cells produced no significant changes in gene expression of i-proteasomal components (Fig. 1B). These negative results were not caused by technical factors, as IMR90 cells showed a strong upregulation of all three i-proteasomal subunits by interferon- γ (4 ng/ml, 24 h: 3.1 ± 0.4 , 49 ± 11.4 and 3.7 ± 0.3 -fold for LMP7, LMP2 and LMP10 respectively, $n = 3$).

FA cytotoxicity. Mutations in i-proteasome proteins result in specific human disorders, however, knockouts of individual i-proteasome genes in mice did not cause any overt pathophysiological changes^{4,5}, suggesting that the absence of i-proteasome proteins leads to compensatory changes. In agreement with pathological phenotypes of mutated i-proteasomes in humans, pharmacological inhibition of i-proteasomes in mice produced clear physiological effects. A selective inhibitor of LMP7 activity, ONX-0914²⁸, is a commonly used tool for interrogation of i-proteasome functions *in vitro* and in animal models of human diseases. Treatments of H460 lung cells with 0.3 or 0.6 μ M ONX-0914 (LMP7-i) resulted in the appearance of a slower moving LMP7 band, which was equivalent to a gain of 0.5–1 kDa (Fig. 2A). The magnitude of the observed shift corresponds to a covalent attachment of a single LMP7-i (581 Da molecular weight). LMP2 showed a larger shift (2.5–3 kDa), corresponding to its unprocessed form, which probably results from the mutually dependent incorporation and activation of i-proteasome components^{29,30}. In agreement with qRT-PCR data (Fig. 1B), FA did not alter protein levels of LMP2 or LMP7 (Fig. 2A). To test LMP7-i effects on the constitutive proteasomes, we measured levels of unstable transcription factors HIF1 α and p53, which both undergo proteasome-dependent degradation in unstressed cells. In contrast to the proteasome inhibitor MG132, LMP7-i had no effect on the stability of HIF1 α and p53 (Fig. 2B). LMP7-i also had no effect on Ser326 phosphorylation of the proteotoxic stress-sensitive transcription factor HSF1, which showed a massive upregulation by MG132. Importantly, the selected dose of our positive control MG132 caused only a partial proteasome inhibition as evidenced by the lack of free ubiquitin depletion (Fig. 2B). The addition of LMP7-i for 6 h produced no changes in cell cycle and DNA replication (Fig. 2C). Longer 24 h incubations with $\geq 0.5 \mu$ M LMP7-i led to modest (15–20%) decreases in the colony formation (Fig. 2D), indicating that i-proteasomes play some role in the normal physiology of H460 cells. The impact of i-proteasomes on FA cytotoxicity was first examined by the clonogenic assay, which integrates all forms of cell death. The presence of LMP7-i during 3 h FA exposures and the subsequent 24 h recovery significantly diminished clonogenic viability of cells (Fig. 2E). Since FA is a potent replication stressor^{26,27}, we also tested cytotoxicity of two other replication stressors hydroxyurea and camptothecin. Hydroxyurea causes stalling of replication forks by depleting cells of dNTPs whereas camptothecin produces DNA-topoisomerase I crosslinks. Unlike FA, cotreatments with LMP7-i and hydroxyurea or camptothecin did not elicit significant changes in clonogenic viability (Fig. 2F,G). Thus, i-proteasomes do not have a general role in cell recovery from replication stress.

Genotoxic signaling by FA. FA conjugates to lysine-rich basic proteins such as histones and i-proteasomes have higher activity on these types of proteins¹⁴. Thus, i-proteasomes could be potentially involved in recovery from FA-histone damage that includes DNA-histone crosslinks and FA-histone modification. FA-induced DPCs and chromatin damage triggered activation of the apical kinases ATR²⁶ and ATM²⁷, respectively. Inhibition of i-proteasomes did not alter phosphorylation of either ATM (CHK2, KAP1) or ATR (CHK1, p53) substrates by FA (Fig. 3A–C). Consistent with the normal activation of p53 (Fig. 3A,C), upregulation of its target, the CDK inhibitor p21, was also unaltered by LMP7-i (Fig. 3C). The presence of LMP7-i during short FA treatments also produced no changes in ATM- or ATR-dependent phosphorylation (Fig. 3D). Ser139-phosphorylated histone H2AX (known as γ -H2AX) is a well-established marker of genotoxic stress³¹. In FA-treated cells, γ -H2AX was found exclusively in S-phase cells and its levels were elevated by inhibition of standard proteasomes³². We confirmed that γ -H2AX was present only in the S-phase, as indicated by identical levels of γ -H2AX-positive and γ -H2AX/EdU double-positive cells (Fig. 3E,F). I-proteasome inactivation did not alter the overall or S-phase-specific formation of γ -H2AX.

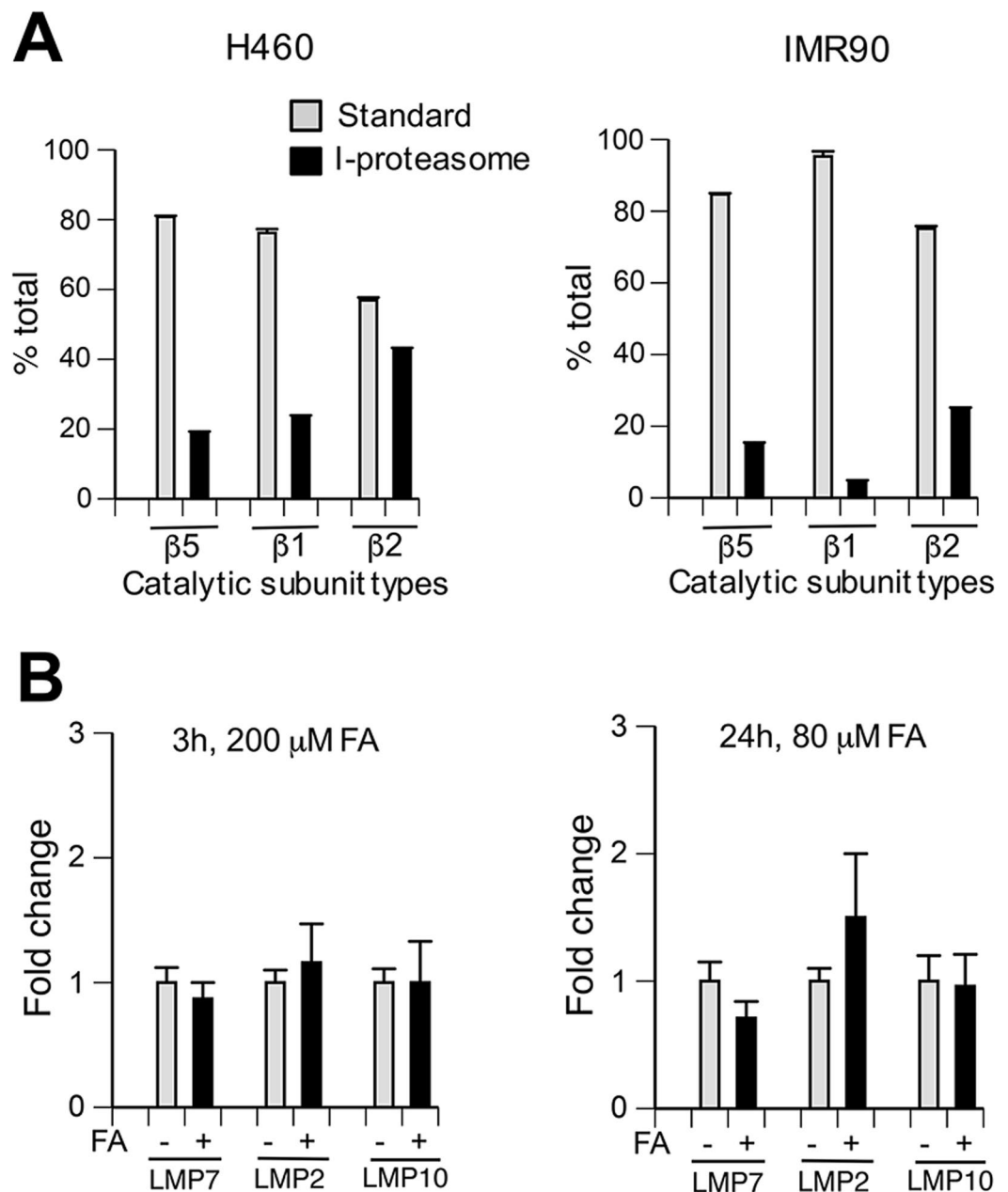


Figure 1. qRT-PCR for catalytic proteasomal subunits. Data are means \pm SD for three independent RNA samples. Where not seen, error bars were smaller than symbols. **(A)** Relative amounts of standard and i-proteasomal subunits within three types of catalytic activities ($\beta 5$: PSMB5 and LMP7, $\beta 2$: PSMB6 and LMP10, $\beta 1$: PSMB7 and LMP2). **(B)** Gene expression of i-proteasome subunits is not altered by FA treatments in normal IMR90 cells.

Caspase activation and cell death. FA-treated H460 cells undergo apoptosis, which is in part mediated by the transcription factor p53²⁶. We found that the FA-induced production of a caspase-generated PARP fragment and cleaved (active) executioner caspase 7 were not affected by i-proteasome inhibition (Fig. 4A,B). LMP7-i activity was not lost during prolonged incubations, as evidenced by the continuing presence of the slower migrating LMP7 form (Fig. 3B). We next investigated LMP7-i effects on survival of cells with blocked caspase activation. We included a previously validated dose of the pancaspase inhibitor Q-VD-Oph³³ during FA treatments and the subsequent 72 h recovery and examined the colony formation. As expected based on the detection of activated caspases, Q-VD-Oph significantly decreased clonogenic toxicity of FA (Fig. 4C). We also found that i-proteasome inhibition enhanced clonogenic toxicity of FA even in the presence of Q-VD-Oph (Fig. 4D). These findings together with the normal activation of the proapoptotic transcription factor p53 (Fig. 3A,C) indicate that i-proteasomes are protective against a caspase-independent cell death.

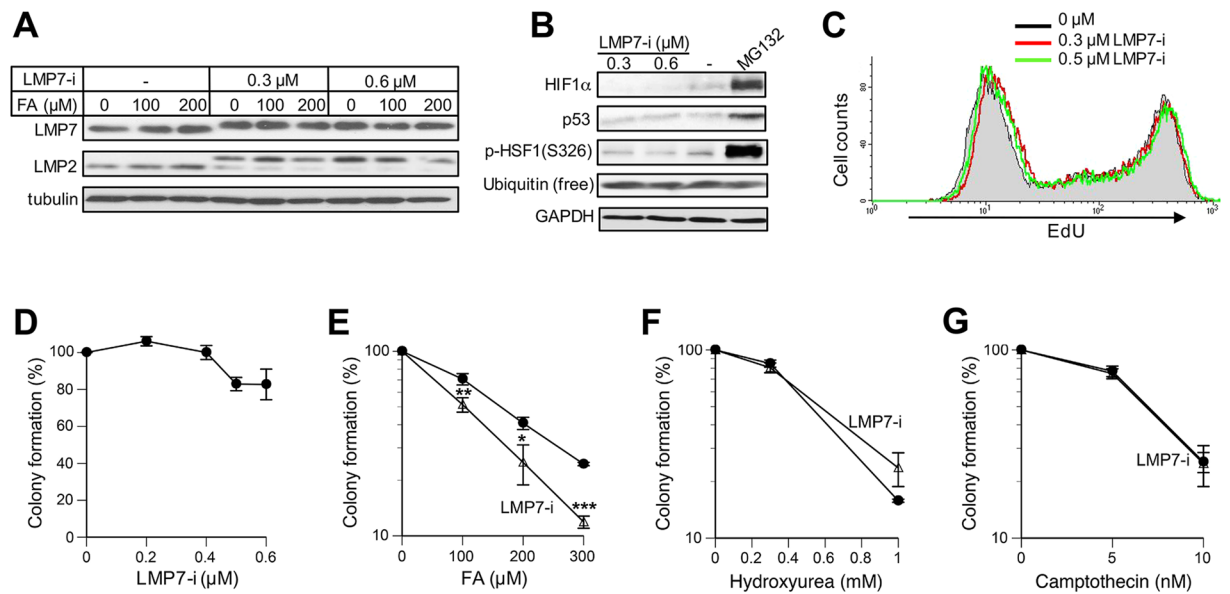


Figure 2. Cytotoxicity of FA and replication stressors in H460 cells. (A) Westerns for LMP2 and LMP7 in cells treated with FA and ONX-0914 (LMP7-i) for 3 h. (B) Westerns for cells treated with LMP7-i and MG132 (5 μ M) for 4 h. (C) FACS profiles of EdU incorporation in cells treated with LMP7-i for 6 h. EdU was added during the last hour. (D) Clonogenic survival of cells treated with LMP7-i for 24 h. (E) Clonogenic survival of cells cotreated with FA and 0.5 μ M LMP7-i for 3 h and then incubated for 24 h with 0.5 μ M LMP7-i (means \pm SD for three experiments in triplicates, * p < 0.05, ** p < 0.01, *** p < 0.001). (F) Clonogenic survival of cells cotreated for 24 h with 0.5 μ M LMP7-i and hydroxyurea or (G) camptothecin (means \pm SD for two experiments in triplicates).

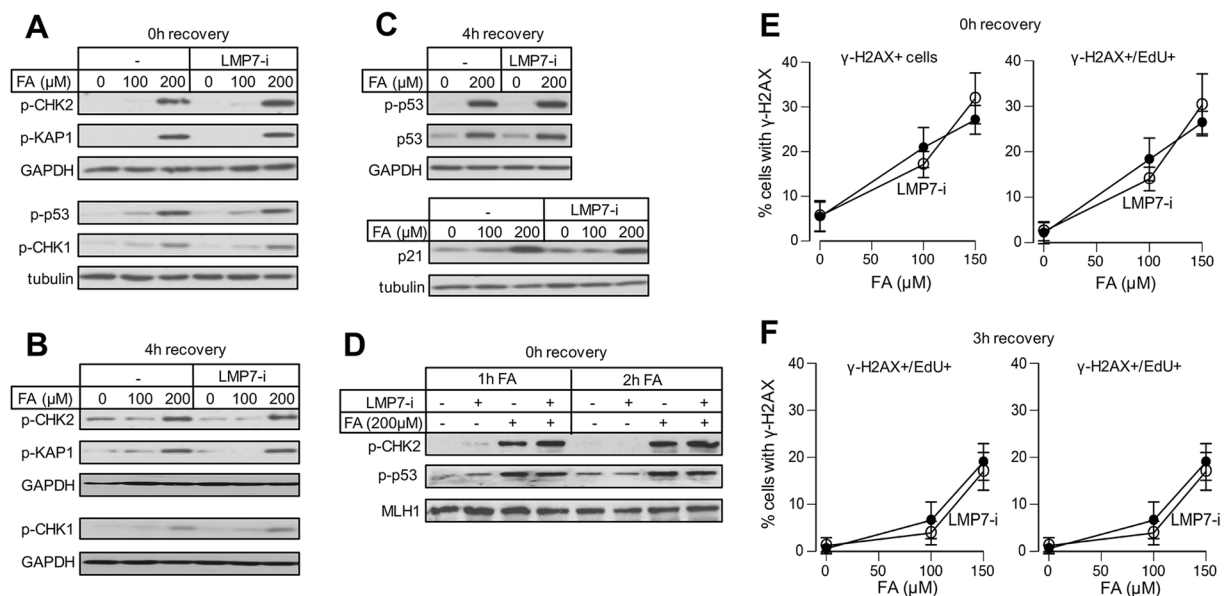


Figure 3. Genotoxic signaling in H460 cells. Cells were treated with FA for 3 h except for panel D. LMP7-i (0.5 μ M) was present during and after FA treatments (p-CHK2, p-CHK1, p-KAP1, p-p53: phosphorylated forms). (A) Genotoxic signaling at 0 h or (B) 4 h recovery after FA exposure. (C) Westerns for markers of p53 activation at 4 h recovery post-FA. (D) Phosphorylation of CHK2 and p53 in cells treated with FA for 1 or 2 h. (E) Percentage of cells containing γ -H2AX foci (γ -H2AX+) and both γ -H2AX foci and EdU staining (γ -H2AX+/EdU+) (means \pm SD, n = 3). (F) As panel E except that cells were fixed at 3 h post-FA exposure (means \pm SD, n = 3).

Stress responses in normal human cells. IMR90 normal lung fibroblasts do not undergo apoptosis after moderate FA doses²⁶, making them well-suited for cell cycle studies. Inhibition of standard proteasomes in these cells increased early genotoxic signaling responses²⁷. The addition of 0.1 or 0.3 μ M LMP7-i completely shifted the

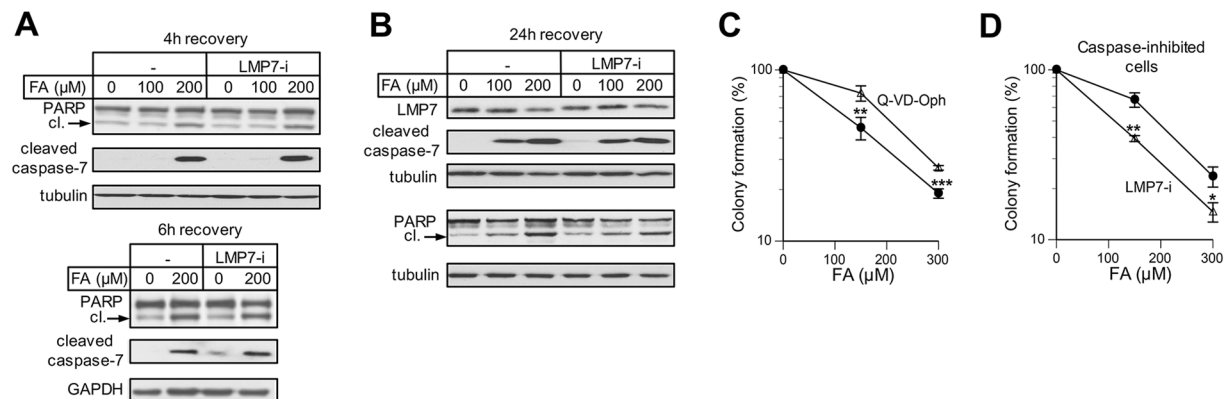


Figure 4. Apoptosis in cells with inactive i-proteasomes. H460 cells were treated with FA for 3 h in the presence or absence of 0.5 μM LMP7-i. The inhibitor was also present during the indicated recovery times. **(A)** Westerns for apoptotic markers at 4 h and 6 h recovery or **(B)** 24 h recovery post-FA treatments (cl.- cleaved PARP). **(C)** Effect of the pancaspase inhibitor Q-VD-Oph (20 μM) on survival of H460 cells. Q-VD-Oph was present during FA treatments and 72 h post-FA (means ± SD, ***p* < 0.01, ****p* < 0.001, *n* = 3). **(D)** Impact of LMP7-i on FA toxicity in the presence of the pancaspase inhibitor Q-VD-Oph (20 μM). LMP7-i was coincubated with FA for 3 h and then added for additional 24 h. Data are means ± SD, **p* < 0.05, ***p* < 0.01, *n* = 3.

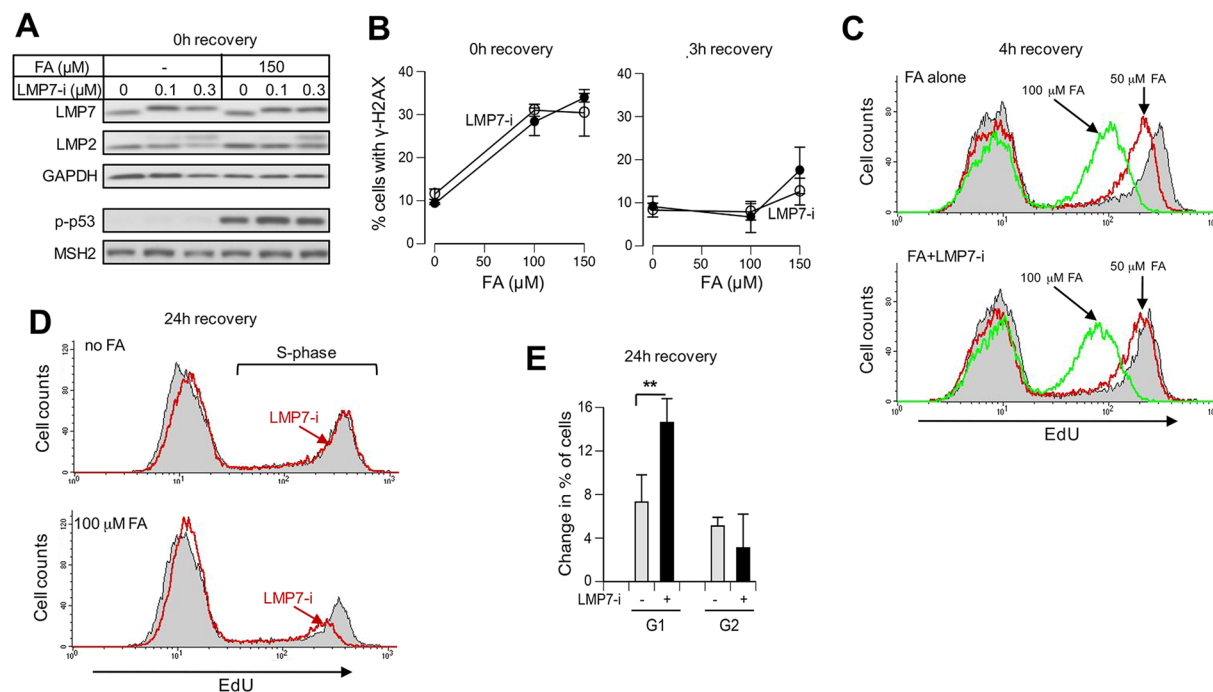


Figure 5. Genotoxic and cell cycle responses in normal human cells. IMR90 cells were treated with FA for 3 h. LMP7-i was present during FA treatments and the subsequent recovery times. EdU was added during the last 1 h of recovery incubations. **(A)** Dose-dependent effects of LMP7-i in cells immediately after FA treatments (p-p53: Ser15-phosphorylated p53). **(B)** Percentage of γ-H2AX-containing cells collected immediately or after 3 h recovery post-FA treatments (*n* = 3). **(C)** FACS profiles of EdU-labeled cells at 4 h or **(D)** 24 h recovery after FA removal. **(E)** FA-induced changes in G1 and G2 phases. Cells were treated with 100 μM FA for 3 h and collected for FACS after 24 h recovery. Statistics: ***p* < 0.01, *n* = 4.

LMP7 band and the higher dose also produced a slower moving LMP2 band (Fig. 5A). In further experiments, we used 0.3 μM LMP7-i in IMR90 cells. Similar to H460, i-proteasome inhibition in IMR90 cells did not alter early genotoxic responses to FA, such as p53 phosphorylation, γ-H2AX production or DNA synthesis (Fig. 5A–C). However, i-proteasome inactivation impaired a long-term recovery of IMR90 cells from FA damage, resulting in the depletion of S-phase (Fig. 5D) and accumulation of G1 cells (Fig. 5E). Thus, i-proteasomes also play a protective role against FA toxicity in primary human cells.

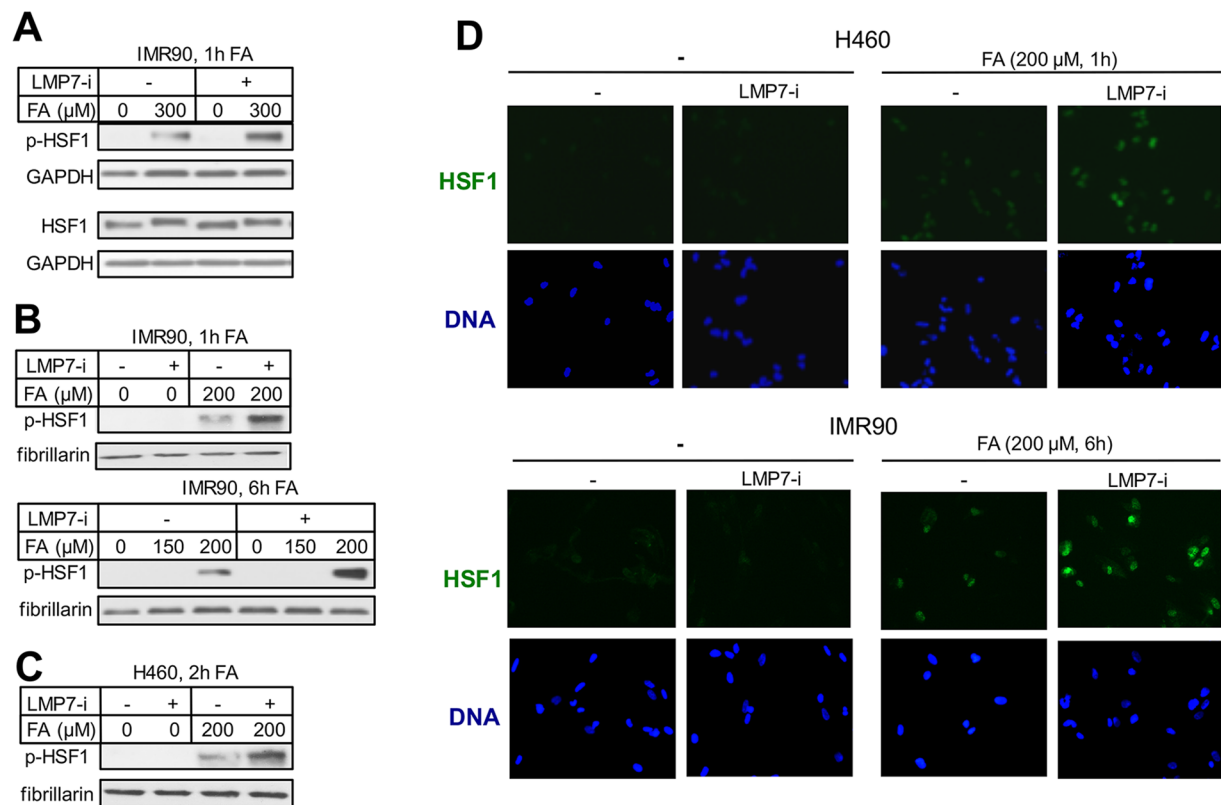


Figure 6. HSF1 activation in cells with inhibited i-proteasomes. Cells were treated with FA in the absence or presence of 0.3 μ M LMP7-i. (A) Westerns for HSF1 and its S326-phosphorylated form (p-HSF1) in whole cell lysates of IMR90 treated with FA for 1 h. (B) S326-phosphorylated HSF1 in the nuclear fraction of IMR90 cells. (C) Nuclei-bound phospho-S326-HSF1 in H460 cells treated with FA for 2 h. (D) Nuclear HSF1 in FA-treated H460 and IMR90 cells. Cells were extracted with 0.2% Triton X-100 in PBS for 10 min at 4 °C before fixation.

HSF1 activation. We have recently identified FA as a potent inducer of the heat shock-responsive transcription factor HSF1²⁴. HSF1 normally resides in the cytosol but accumulation of misfolded proteins induces its phosphorylation, nuclear translocation and binding to chromatin³⁴. We first examined HSF1-Ser326 phosphorylation, which has shown a robust dose-dependent response to FA²⁴. I-proteasome inhibition strongly enhanced Ser326 phosphorylation by FA in IMR90 cells whereas HSF1 protein levels remained unchanged (Fig. 6A). A slower mobility of HSF1 in FA samples is typical for proteotoxic conditions and reflects its phosphorylation at multiple sites³⁴. FA-treated IMR90 and H460 cells with inactive i-proteasomes also showed higher amounts of nuclear Ser326-phosphorylated (Fig. 6B,C) and total HSF1 (Fig. 6D). Overall, these results indicate elevated levels of FA-induced proteotoxic stress in cells with disabled i-proteasomes.

Native gel analysis of proteasomes. A native gel electrophoresis allows separation of 20S and 26S particles that are subsequently identified by western blotting for their specific components³⁵. We found that a majority of standard core 20S particles (~65%), detected by the presence of the chymotrypsin-like protease PSMB5, was uncapped in control H460 and IMR90 cells (Fig. 7A). These values are consistent with the results in other mammalian cells³. In response to FA, incorporation of regular 20S particles into capped 26S proteasomes slightly decreased in H460 (from 36.6 \pm 3.5% to 30.1 \pm 1.5%) but remained the same in IMR90 cells (36.1 \pm 2.2% for control *versus* 35.5 \pm 0.4% for FA). Similar to constitutive 20S proteasomes, a majority of 20S i-proteasomes identified by immunoblotting for LMP7 that replaces PSMB5 in i-proteasomes was also uncapped in control cells (Fig. 7B). Unexpectedly, we found that FA caused severe losses of 26S i-proteasomes in both H460 and IMR90 cells. The overall LMP7 protein amounts were not altered by FA treatments (Fig. 7C). All 19S particles detected by its base component Rpt2 were incorporated into 26S proteasomes irrespective of FA treatments in H460 cells (Fig. 7D). In primary IMR90 cells, 19S proteasomes were present in both free and 26S forms and their distribution was not noticeably altered by FA. Thus, 26S i-proteasomes but not standard 26S proteasomes were sensitive to FA-induced disassembly. Proteolytic activity of 20S core particles is promoted by their association with small PA28 (11S) activators: cytoplasmic PA28 $\alpha\beta$ and nuclear PA28 γ^3 . PA28 $\alpha\beta$ is particularly important for stimulation of 20S i-proteasomes. We found that FA increased by approximately 2-fold a fraction of PA28 $\alpha\beta$ that was bound to 20S particles (74.8 \pm 2.8% from 36.2 \pm 2.8 in controls, n = 2, p = 0.027) (Fig. 7E, left panel). A similar change was found when 20S-bound PA28 $\alpha\beta$ was normalized to the amount of the 20S component PSMB5 (1.9-fold increase by FA). FA also induced a higher association of PA28 γ with 20S particles (Fig. 7E, right panel) although the fraction of 20S-bound PA28 γ was lower than that for PA28 $\alpha\beta$.

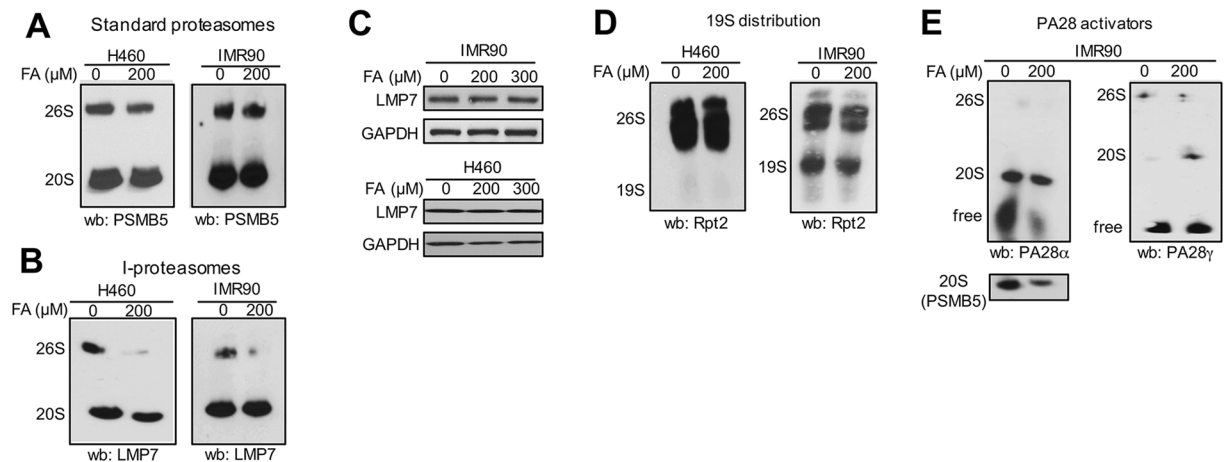


Figure 7. Native gel electrophoresis of proteasomes. H460 and IMR90 cells were treated with 200 μM FA for 2 h. **(A)** Distribution of standard 20S proteasomes between free and 19S-capped (26S) forms. **(B)** I-proteasome distribution between free (20S) and 19S-capped (26S) forms. **(C)** LMP7 levels in control and FA-treated cells. **(D)** Distribution of 19S proteasome between its free and 26S-bound forms. **(E)** Proteasome binding of small activators PA28 α (left panel) and PA28 γ (right panel).

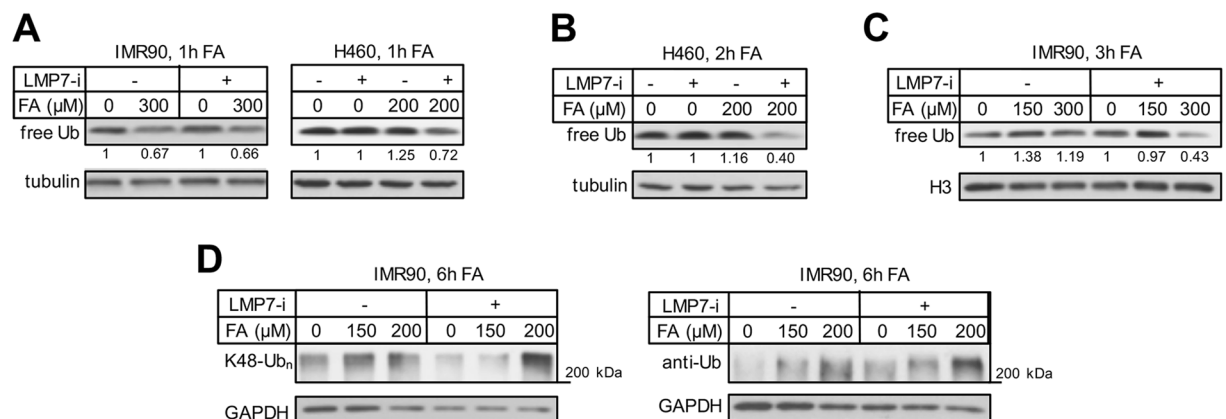


Figure 8. Ubiquitin reserves and protein polyubiquitination. Panels A–C: whole cell lysates were used for westerns and LMP7-i was added at 0.3 μM . **(A)** Free ubiquitin in cells treated with FA for 1 h with and without LMP7-i. **(B)** Free ubiquitin in H460 cells treated with FA +/- LMP7-i for 2 h and **(C)** IMR90 cells treated with FA +/- LMP7-i for 3 h. **(D)** K48-linked (K48-Ub_n) and overall polyubiquitination (anti-Ub) of cytoplasmic proteins in IMR90 cells treated with FA +/- LMP7-i (0.2 μM) for 6 h.

Ubiquitin reserves and protein polyubiquitination. The disassembly of 26S i-proteasomes and the increased association of PA28 activators with 20S particles indicate a shift towards ubiquitin-independent proteolysis. This raises the question whether cells with inactivated i-proteasomes experience a higher stress on the ubiquitin system due to the need for ubiquitination of additional proteins for destruction by standard 26S proteasomes. One measure of ubiquitin usage is the amount of free ubiquitin³⁶. Inhibition of i-proteasomes during 1 h FA treatments produced either no impact (IMR90 cells) or only a modest depletion of free ubiquitin (H460 cells) (Fig. 8A). The inactivity of i-proteasomes during longer FA incubations caused >2-fold depletion of free ubiquitin, which showed no changes in cells with functional i-proteasomes (Fig. 8B,C). Consistent with the dynamics of free ubiquitin, cells with disabled i-proteasomes contained higher levels of polyubiquitinated cytoplasmic proteins as detected with two antibodies (Fig. 8D).

Discussion

In this work we obtained evidence for the importance of i-proteasome activity in recovery of human cells from injury by carcinogenic FA. Previous studies have found altered FA cytotoxicity in cells with certain DNA repair deficiencies, demonstrating the toxicological significance of DNA damage^{37–39}. DPCs are generally considered as the main form of FA-induced DNA damage^{15,21}. DPC repair involves a proteolytic removal of crosslinked proteins, which can be performed by a DNA-dependent protease SPRTN in conjunction with DNA replication^{40,41}.

Inhibition of the constitutive proteasomes has also impaired removal of FA-produced DPCs in human cells⁴² and altered genotoxic signaling responses in a manner that was consistent with a diminished repair of DPCs³². Histones are the main nuclear proteins modified by FA due to its high reactivity with the side-chain amino group of lysine. Chromatin damage by FA without the involvement of DNA also triggers activation of the genotoxic stress-sensitive kinase ATM²⁷. Although i-proteasomes exhibit a higher activity towards basic proteins such as histones¹⁴, the protective function of i-proteasomes against FA did not result from their involvement in repair of chromatin or DNA. This conclusion is supported by several experimental observations. FA-induced DPCs are potent blockers of DNA replication^{26,27} due to the inability of the ring-shaped replicative helicase complexes to progress over the steric block imposed by the bulkiness of DPCs⁴³. Our results on the normal recovery of DNA synthesis and the normal formation and decay of the genotoxic stress marker γ -H2AX in cells with suppressed i-proteasome activity indicate that the removal of replication-blocking FA-DNA lesions was not affected. The presence of unrepaired DPCs leads to accumulation of cells in the G2 phase, which was not observed in FA-treated cells with inactivated i-proteasomes in contrast to inhibition of standard proteasomes³². FA-triggered DNA damage signaling responses include DPC-linked phosphorylation of CHK1 and p53 by ATR²⁶ and chromatin damage-induced CHK2 and KAP1 phosphorylation by ATM²⁷. None of these signaling responses were altered by i-proteasome inhibition, further strengthening the argument that the prosurvival role of i-proteasomes involved cellular recovery from nongenotoxic injury by FA.

We have recently found that FA induces proteolytic polyubiquitination of proteins throughout the cell, especially in the cytoplasm, and causes a rapid activation of the cytosolic protein damage sensor HSF1²⁴. Elevated levels of the activating Ser326 phosphorylation and chromatin binding of HSF1 in cells with inhibited LMP7 indicate that i-proteasome activity was probably most important for removal of FA-damaged cytosolic proteins. This suggestion is further supported by higher amounts of polyubiquitinated cytoplasmic proteins in cells with disabled i-proteasomes. FA caused a near complete release of the catalytic 20S i-proteasome from 26S i-proteasomes but little or no dissociation of standard 26S proteasomes, indicating that i-proteasome activity was shifted from ubiquitin-dependent to ubiquitin-independent proteolysis. Suppression of i-proteasome activity showed a greater usage of ubiquitin in FA-treated cells, pointing to a larger burden of proteins that required ubiquitination. The switch to ubiquitin-independent proteolysis of FA-damaged proteins benefits stressed cells by saving ubiquitin for tagging and proteolysis of other proteins and preserving ATP due to energy independence of 20S-mediated protein degradation. There are no other reports on a stress-induced disassembly of 26S i-proteasomes although the dissociation of standard 26S proteasomes is a known protective response against oxidized proteins^{12,44}. Oxidation of protein cysteines⁴⁵ and the protein chaperone HSP70⁴⁶ have been implicated in the destabilization of standard 26S proteasomes by oxidative stress. It is possible that similar processes are involved in the disassembly of 26S i-proteasomes by FA, which reacts with NH₂/SH-groups resulting in the formation of damaged/misfolded proteins that can titrate HSP70 away from 26S i-proteasome promoting dissociation of the regulatory 19S particle. The typical substrates for ubiquitin-independent proteolysis in unstressed cells are intrinsically unstable or unstructured proteins^{3,12}, suggesting that these proteins could be particularly vulnerable to misfolding in response to chemical modifications of Lys and Cys by FA. The conformational flexibility of unstructured polypeptides can bring reactive Cys/Lys in a close proximity, allowing FA-induced crosslinking of two amino acids and thereby fixing distorted structures. When not promptly removed, severely misfolded proteins form aggregates that are resistant to proteasome-mediated proteolysis and can exert chronic toxic effects¹. This pathological mechanism can explain delayed cell cycle abnormalities caused by i-proteasome inhibition in FA-damaged cells.

Methods

Chemicals. ONX-0914 (A4011) and Q-VD-Oph (A1901) were from ApexBio. Formaldehyde (F8775), camptothecin (C9911) and hydroxyurea (H8627) were from Sigma. Interferon- γ was purchased from Thermo Scientific (RIFNG50).

Cells and treatments. H460 and IMR90 cells were purchased from the American Type Culture Collection and cultured as previously described²⁷. Cells were treated with FA and other stressors in complete growth media. ONX-0914 (LMP7-i) was added to cells 1 h before FA and present during FA treatments. For induction of i-proteasomes, cells were treated with 4 ng/ml interferon- γ for 24 h.

Western blotting. Whole cell lysates, cytoplasmic extracts and insoluble nuclear fractions were prepared as recently described²⁴. Unless specified otherwise, western blots were run using whole cell lysates. Proteins were separated by SDS-PAGE and immobilized on PVDF membranes. The following primary antibodies were used: LMP2 (sc-37397, Santa Cruz), phospho-S824-KAP1 (A300-767-A, Bethyl); LMP7 (13635), ubiquitin (3933), K48-linked polyubiquitin (5621), HSF1 (4356), PSMB5 (11903), phospho-S317-CHK1 (2344), phospho-T68-CHK2 (2661), phospho-S15-p53 (9284) from Cell Signaling; Rpt2 (ab20239) and phospho-S326-HSF1 (ab76076) from Abcam. Other antibodies were described previously⁴⁷.

Native gel electrophoresis. Cells were resuspended in a proteasome extraction buffer (50 mM Tris-HCl, pH 8.0, 5 mM MgCl₂, 0.5 mM EDTA, 1 mM ATP and protease and phosphatase inhibitors) and vortexed for 5 min at 4 °C with acid-washed glass beads (Sigma, G1145). The proteasome-containing supernatants were collected after centrifugation at 15000 g for 15 min, 4 °C. Native electrophoresis was performed on 4% polyacrylamide gels³⁵.

Microscopy. Immunostaining protocols for nuclear HSF1²⁴ and phospho-H2AX⁴⁸ have been described earlier. S-phase cells were labeled with 10 μ M 5-ethynyl-2'-deoxyuridine (EdU) for 1 h prior to the addition of FA. Primary antibodies were rabbit polyclonal anti-HSF1 (4356S, Cell Signaling) and rabbit polyclonal anti-phospho-histone H2AX (06-570, Millipore). Antibodies were diluted in a PBS solution containing 1% BSA

and 0.5% Tween-20 and incubated with cells for 2 h at 37 °C. Images were acquired on the Nikon E-800 Eclipse fluorescent microscope.

Cell cycle analysis. A recently described procedure was followed³². DNA synthesis was measured by EdU labeling (10 μM, 1 h). DNA ploidy was determined by propidium iodide staining (40 μg/ml, 30 min at room temperature). Flow cytometry data were acquired on FACSCalibur (BD Biosciences) and analyzed by the CellQuest Pro software.

Clonogenic survival. H460 cells were seeded onto 60-mm dishes (400 cells/dish) and treated with chemicals on the next day. After 6–8 days of growth, colonies were fixed with methanol and stained with the Giemsa solution.

qRT-PCR. Total cellular RNA was purified with TRIzol Reagent (Ambion) and used for reverse transcription reaction (RT First Strand Kit, Qiagen). Real-Time PCR reactions were prepared using the RT SYBR Green ROX qPCR Mastermix and primers from Qiagen and run on the ViiA7 Real-Time PCR System (Applied Biosystems). Expression of i-proteasome subunits after FA treatments was determined by the $\Delta\Delta C_t$ method using B2M, GAPDH and TBP mRNAs for normalization. Calculations of the relative gene expression for catalytic subunits within the same type of activity ($\beta 1$, $\beta 2$ or $\beta 5$) included the following steps: 1) determination of the ratio (Ri) of the i-proteasome subunit expression to the standard subunit expression by subtracting the corresponding C_t values and using the resulting number as the power in the binary logarithm and 2) determination of the percentage of the i-proteasome subunit using the following equation: $(Ri/1 + Ri) \times 100\%$. The overall percentage of i-proteasomes was calculated by combining individual percentages for $\beta 1i$, $\beta 2i$ and $\beta 5i$ subunits and dividing by 3.

Statistics. Two-tailed, unpaired *t*-test was used for the evaluation of statistical differences between the groups.

References

- Morimoto, R. I. Proteotoxic stress and inducible chaperone networks in neurodegenerative disease and aging. *Genes Dev* **22**, 1427–38 (2008).
- Livneh, I., Cohen-Kaplan, V., Cohen-Rosenzweig, C., Avni, N. & Ciechanover, A. The life cycle of the 26S proteasome: from birth, through regulation and function, and onto its death. *Cell Res* **26**, 869–85 (2016).
- Ben-Nissan, G. & Sharon, M. Regulating the 20S proteasome ubiquitin-independent degradation pathway. *Biomolecules* **4**, 862–84 (2014).
- Yewdell, J. W. Immunoproteasomes: regulating the regulator. *Proc Natl Acad Sci USA* **102**, 9089–90 (2005).
- Ferrington, D. A. & Gregerson, D. S. Immunoproteasomes: structure, function, and antigen presentation. *Prog Mol Biol Transl Sci* **109**, 75–112 (2012).
- Deol, P., Zaiss, D. M., Monaco, J. J. & Sijts, A. J. Rates of processing determine the immunogenicity of immunoproteasome-generated epitopes. *J Immunol* **178**, 7557–62 (2007).
- Toes, R. E. *et al.* Discrete cleavage motifs of constitutive and immunoproteasomes revealed by quantitative analysis of cleavage products. *J Exp Med* **194**, 1–12 (2001).
- Hussong, S. A., Kapphahn, R. J., Phillips, S. L., Maldonado, M. & Ferrington, D. A. Immunoproteasome deficiency alters retinal proteasome's response to stress. *J Neurochem* **113**, 1481–90 (2010).
- Ferrington, D. A. *et al.* Immunoproteasome responds to injury in the retina and brain. *J Neurochem* **106**, 158–69 (2008).
- Diaz-Hernandez, M. *et al.* Neuronal induction of the immunoproteasome in Huntington's disease. *J Neurosci* **23**, 11653–61 (2003).
- Kotamraju, S. *et al.* Upregulation of immunoproteasomes by nitric oxide: potential antioxidative mechanism in endothelial cells. *Free Radic Biol Med* **40**, 1034–44 (2006).
- Pickering, A. M. *et al.* The immunoproteasome, the 20S proteasome and the PA28 α proteasome regulator are oxidative-stress-adaptive proteolytic complexes. *Biochem J* **432**, 585–94 (2010).
- Seifert, U. *et al.* Immunoproteasomes preserve protein homeostasis upon interferon-induced oxidative stress. *Cell* **142**, 613–24 (2010).
- Raule, M., Cerruti, F. & Cascio, P. Enhanced rate of degradation of basic proteins by 26S immunoproteasomes. *Biochim Biophys Acta* **1843**, 1942–7 (2014).
- NTP (National Toxicology Program). Final Report on Carcinogens Background Document for Formaldehyde. *Rep. Carcinog. Backgr* **10-5981** (2010).
- Oberbeck, N. *et al.* Maternal aldehyde elimination during pregnancy preserves the fetal genome. *Mol Cell* **55**, 807–17 (2014).
- Pontel, L. B. *et al.* Endogenous Formaldehyde Is a Hematopoietic Stem Cell Genotoxin and Metabolic Carcinogen. *Mol Cell* **60**, 177–88 (2015).
- Paasma, R., Hovda, K. E. & Jacobsen, D. Methanol poisoning and long term sequelae - a six years follow-up after a large methanol outbreak. *BMC Clin Pharmacol* **9**, 5 (2009).
- Reddy, N. J., Sudini, M. & Lewis, L. D. Delayed neurological sequelae from ethylene glycol, diethylene glycol and methanol poisonings. *Clin Toxicol (Phila)* **48**, 967–73 (2010).
- Hecht, S. S. Tobacco carcinogens, their biomarkers and tobacco-induced cancer. *Nat Rev Cancer* **3**, 733–44 (2003).
- IARC (International Agency for Research on Cancer). Formaldehyde. *IARC Monogr. Eval. Carcinog. Risks Hum.* **88**, 39–325 (2006).
- Hauptmann, M. *et al.* Mortality from lymphohematopoietic malignancies and brain cancer among embalmers exposed to formaldehyde. *J Natl Cancer Inst* **101**, 1696–708 (2009).
- Schwilk, E., Zhang, L., Smith, M. T., Smith, A. H. & Steinmaus, C. Formaldehyde and leukemia: an updated meta-analysis and evaluation of bias. *J Occup Environ Med* **52**, 878–86 (2010).
- Ortega-Atienza, S., Rubis, B., McCarthy, C. & Zhitkovich, A. Formaldehyde Is a Potent Proteotoxic Stressor Causing Rapid Heat Shock Transcription Factor 1 Activation and Lys48-Linked Polyubiquitination of Proteins. *Am J Pathol* **186**, 2857–2868 (2016).
- Lu, Z., Li, C. M., Qiao, Y., Yan, Y. & Yang, X. Effect of inhaled formaldehyde on learning and memory of mice. *Indoor Air* **18**, 77–83 (2008).
- Wong, V. C., Cash, H. L., Morse, J. L., Lu, S. & Zhitkovich, A. S-phase sensing of DNA-protein crosslinks triggers TopBP1-independent ATR activation and p53-mediated cell death by formaldehyde. *Cell Cycle* **11**, 2526–37 (2012).
- Ortega-Atienza, S., Wong, V. C., DeLoughery, Z., Luczak, M. W. & Zhitkovich, A. ATM and KAT5 safeguard replicating chromatin against formaldehyde damage. *Nucleic Acids Res* **44**, 198–209 (2016).
- Muchamuel, T. *et al.* A selective inhibitor of the immunoproteasome subunit LMP7 blocks cytokine production and attenuates progression of experimental arthritis. *Nat Med* **15**, 781–7 (2009).

29. Groettrup, M., Standera, S., Stohwasser, R. & Kloetzel, P. M. The subunits MECL-1 and LMP2 are mutually required for incorporation into the 20S proteasome. *Proc Natl Acad Sci USA* **94**, 8970–5 (1997).
30. Griffin, T. A. *et al.* Immunoproteasome assembly: cooperative incorporation of interferon gamma (IFN-gamma)-inducible subunits. *J Exp Med* **187**, 97–104 (1998).
31. Scully, R. & Xie, A. Double strand break repair functions of histone H2AX. *Mutat Res* **750**, 5–14 (2013).
32. Ortega-Atienza, S., Green, S. E. & Zhitkovich, A. Proteasome activity is important for replication recovery, CHK1 phosphorylation and prevention of G2 arrest after low-dose formaldehyde. *Toxicol Appl Pharmacol* **286**, 135–41 (2015).
33. Green, S. E., Luczak, M. W., Morse, J. L., DeLoughery, Z. & Zhitkovich, A. Uptake, p53 pathway activation, and cytotoxic responses for Co(II) and Ni(II) in human lung cells: implications for carcinogenicity. *Toxicol Sci* **136**, 467–77 (2013).
34. Anckar, J. & Sistonen, L. Regulation of HSF1 function in the heat stress response: implications in aging and disease. *Annu Rev Biochem* **80**, 1089–115 (2011).
35. Elsasser, S., Schmidt, M. & Finley, D. Characterization of the proteasome using native gel electrophoresis. *Methods Enzymol* **398**, 353–63 (2005).
36. Dantuma, N. P., Groothuis, T. A., Salomons, F. A. & Neeffes, J. A dynamic ubiquitin equilibrium couples proteasomal activity to chromatin remodeling. *J Cell Biol* **173**, 19–26 (2006).
37. Ridpath, J. R. *et al.* Cells deficient in the FANC/BRCA pathway are hypersensitive to plasma levels of formaldehyde. *Cancer Res* **67**, 11117–22 (2007).
38. de Graaf, B., Clore, A. & McCullough, A. K. Cellular pathways for DNA repair and damage tolerance of formaldehyde-induced DNA-protein crosslinks. *DNA Repair (Amst)* **8**, 1207–14 (2009).
39. Rosado, I. V., Langevin, F., Crossan, G. P., Takata, M. & Patel, K. J. Formaldehyde catabolism is essential in cells deficient for the Fanconi anemia DNA-repair pathway. *Nat Struct Mol Biol* **18**, 1432–4 (2011).
40. Vaz, B. *et al.* Metalloprotease SPRTN/DVC1 Orchestrates Replication-Coupled DNA-Protein Crosslink Repair. *Mol Cell* **64**, 704–719 (2016).
41. Stingle, J. *et al.* Mechanism and Regulation of DNA-Protein Crosslink Repair by the DNA-Dependent Metalloprotease SPRTN. *Mol Cell* **64**, 688–703 (2016).
42. Quievryn, G. & Zhitkovich, A. Loss of DNA-protein crosslinks from formaldehyde-exposed cells occurs through spontaneous hydrolysis and an active repair process linked to proteasome function. *Carcinogenesis* **21**, 1573–80 (2000).
43. Duxin, J. P., Dewar, J. M., Yardimci, H. & Walter, J. C. Repair of a DNA-protein crosslink by replication-coupled proteolysis. *Cell* **159**, 346–57 (2014).
44. Wang, X., Yen, J., Kaiser, P. & Huang, L. Regulation of the 26S proteasome complex during oxidative stress. *Sci Signal* **3**, ra88 (2010).
45. Livnat-Levanon, N. *et al.* Reversible 26S proteasome disassembly upon mitochondrial stress. *Cell Rep* **7**, 1371–80 (2014).
46. Grune, T. *et al.* HSP70 mediates dissociation and reassociation of the 26S proteasome during adaptation to oxidative stress. *Free Radic Biol Med* **51**, 1355–64 (2011).
47. Wong, V. C., Morse, J. L. & Zhitkovich, A. p53 activation by Ni(II) is a HIF-1alpha independent response causing caspases 9/3-mediated apoptosis in human lung cells. *Toxicol Appl Pharmacol* **269**, 233–9 (2013).
48. DeLoughery, Z., Luczak, M. W., Ortega-Atienza, S. & Zhitkovich, A. DNA double-strand breaks by Cr(VI) are targeted to euchromatin and cause ATR-dependent phosphorylation of histone H2AX and its ubiquitination. *Toxicol Sci* **143**, 54–63 (2015).

Acknowledgements

This work was supported by grant ES020689 from the National Institute of Environmental Health Sciences.

Author Contributions

Performed experiments: S.O.A., C.K., L.W., C.M. and L.M.W., analyzed data: S.O.A., C.K., L.W., C.M., L.M.W. and A.Z., wrote the paper: S.O.A. and A.Z., designed the overall strategy: A.Z., reviewed and edited the manuscript: all authors.

Additional Information

Competing Interests: The authors declare that they have no competing interests.

Publisher's note: Springer Nature remains neutral with regard to jurisdictional claims in published maps and institutional affiliations.



Open Access This article is licensed under a Creative Commons Attribution 4.0 International License, which permits use, sharing, adaptation, distribution and reproduction in any medium or format, as long as you give appropriate credit to the original author(s) and the source, provide a link to the Creative Commons license, and indicate if changes were made. The images or other third party material in this article are included in the article's Creative Commons license, unless indicated otherwise in a credit line to the material. If material is not included in the article's Creative Commons license and your intended use is not permitted by statutory regulation or exceeds the permitted use, you will need to obtain permission directly from the copyright holder. To view a copy of this license, visit <http://creativecommons.org/licenses/by/4.0/>.

© The Author(s) 2017